

# Ionization and dissociation equilibrium in strongly-magnetized helium atmosphere

Kaya Mori<sup>1,2</sup> and Jeremy S. Heyl<sup>3</sup>

## ABSTRACT

Recent observations and theoretical investigations of neutron stars indicate that their atmospheres consist not of hydrogen or iron but possibly heavier elements such as helium. We calculate the ionization and dissociation equilibrium of helium in the conditions found in the atmospheres of magnetized neutron stars. For the first time this investigation includes the internal degrees of freedom of the helium molecule. We found that at the temperatures and densities of neutron star atmospheres the roto-vibrational excitations of helium molecules are populated. Including these excitations increases the expected abundance of molecules by up to two orders of magnitude relative to calculations that ignore the internal states of the molecule; therefore, if the atmospheres of neutron stars indeed consist of helium, helium molecules and possibly polymers will make the bulk of the atmosphere and leave signatures on the observed spectra from neutron stars.

*Subject headings:* stars: neutron — stars: magnetic fields — stars: atmospheres

## 1. Introduction

Hydrogen has been considered as the surface composition of isolated neutron stars (INSs) because gravitational stratification forces the lightest element to the top of the atmosphere (Alcock & Illarionov 1980). Only a tiny amount of hydrogen is required to constitute an optically thick layer on the surface (Romani 1987). However, recent studies of Chang et al. (2004) and Chang & Bildsten (2004) have shown that the NS surface may be composed

---

<sup>1</sup>Department of Astronomy and Astrophysics, University of Toronto, 50 St. George Street, Toronto, Ontario, M5S 3H4, Canada; mori@astro.utoronto.ca

<sup>2</sup>Canadian Institute for Theoretical Astrophysics, University of Toronto, 60 St. George Street, Toronto, Ontario, M5S 3H8, Canada

<sup>3</sup>Department of Physics and Astronomy; University of British Columbia; Vancouver, BC V6T 1Z1, Canada; Canada Research Chair; hey@physics.ubc.ca

of helium or heavier elements since hydrogen may be quickly depleted by diffusive nuclear burning. Observationally, helium and heavier element atmospheres have been proposed for interpreting the spectral features observed in several INS partially because the existing hydrogen atmosphere models do not reproduce the observed spectra (Sanwal et al. 2002; Hailey & Mori 2002; van Kerkwijk & Kaplan 2006). However, atomic and molecular data in the strong magnetic field regime are scarce for non-hydrogenic elements. Accurate atomic and molecular data are available mostly for the  $\text{He}^+$  ion (Pavlov & Bezchastnov 2005), the helium atom (Neuhauser et al. 1987; Demeur et al. 1994) and  $\text{He}_2^{3+}$  (Turbiner et al. 2006). Helium molecular binding energies have been crudely calculated by density functional theory (Medin & Lai 2006a,b) (hereafter ML06). Unlike hydrogen atmospheres (Lai & Salpeter 1997), the ionization and dissociation balance in strongly-magnetized helium atmosphere has not been investigated yet.

In this paper, we extend our Hartree-Fock type calculation (Mori & Hailey 2002) to helium molecules in the Born-Oppenheimer approximation. We achieved  $\sim 1\%$  and  $\sim 10\%$  accuracy in binding energies and vibrational energies in comparison with the previous studies mainly on hydrogen molecules. Including numerous electronic, vibrational and rotational states, we studied ionization and dissociation equilibrium in helium atmospheres at  $B = 10^{12}\text{--}10^{14}$  G. We also applied our calculations to several INSs which may have helium atmospheres on their surfaces.

## 2. Molecular binding and vibrational energy

At first we adopt the Born-Oppenheimer approximation and neglected any effects associated with motion of atoms and molecules in a magnetic field. Later, we will discuss how the finite nuclear mass modifies results. In the Landau regime ( $\beta > 1$  where  $\beta = B/(4.7 \times 10^9 \text{ G})$ ), bound electrons in an atom and molecule are well specified by two quantum numbers  $(m, \nu)$ .  $m$  is the positive value of a magnetic quantum number and  $\nu$  is a longitudinal quantum number along the field line. We consider only tightly-bound states with  $\nu = 0$ . Electronic excited states with  $\nu > 0$  have small binding energies therefore their population in the atmosphere is tiny due to small Boltzmann factors and pressure ionization. Hereafter we denote atomic and molecular energy states as  $(m_1, m_2, m_3, m_4, \dots)$ . We extend our calculation up to  $B = 10^{14}$  G as relativistic corrections to binding energies are negligible even at  $B > B_Q = 4.4 \times 10^{13}$  G (Angelie & Deutch 1978; Lai 2001).

We computed molecular binding energies with a simple modification to our Hartree-Fock type calculation for atoms (Mori & Hailey 2002). We replaced the nuclear Coulomb term

$V_m(z)$  in the Schrödinger equation by (Lai et al. 1992)

$$\tilde{V}_m(z) = V_m\left(z - \frac{a}{2}\right) + V_m\left(z + \frac{a}{2}\right) \quad (1)$$

where

$$V_m(z) \equiv \int d^2\vec{r}_\perp \frac{|\Phi_m(\vec{r}_\perp)|^2}{r}. \quad (2)$$

The function  $\Phi_m$  is the ground state Landau wavefunction, and  $a$  is the separation between two nuclei. We added  $\frac{Z^2e^2}{a}$  as the Coulomb repulsion energy between the two nuclei. We computed binding energies with a grid size  $\Delta a \sim 0.1$  [a.u.] up to  $a \sim 1$  [a.u.] and  $\Delta a \sim 0.01$  [a.u.] near the energy minimum. Figure 1 shows the binding energy curve of  $\text{He}_2$  at  $B = 10^{12}$  G fitted with the Morse function defined as (Morse 1929)

$$U(a) = \tilde{D}_m \{1 - \exp[-\beta(a - a_0)]\}^2 - E_m \quad (3)$$

where  $E_m (> 0)$  is the molecular binding energy for an electronic state  $m$  (in this paper this usually denotes the magnetic quantum number of the outermost electron),  $a_0$  is the separation between two nuclei at the minimum energy. We defined two different dissociation energies:  $D_m \equiv E_m - 2E_a(gs)$  and  $\tilde{D}_m \equiv E_m - E_a(m_a, m_b) - E_a(m_c, m_d)$ .  $E_a(gs)$  is the ground state energy of an atom (e.g.,  $(0, 1)$  state for Helium atom) and  $E_a(m_a, m_b)$  is the energy of an atom in the  $(m_a, m_b)$  state. Each of the atomic  $m$  quantum numbers  $(m_a, m_b, m_c, m_d)$  corresponds to one of the molecular  $m$  quantum numbers  $(m_1, m_2, m_3, m_4)$  so that  $E_a(m_a, m_b) + E_a(m_c, m_d)$  is the smallest. For instance, helium atoms in  $(0, 3)$  and  $(1, 2)$  state are the least bound system into which  $\text{He}_2$  in the ground state (i.e.  $(0, 1, 2, 3)$  state) will dissociate. Note that a molecule dissociates to atoms and ions when  $E_m < 2E_a(gs)$ , while the molecular binding energy approaches  $E_a(m_a, m_b) + E_a(m_c, m_d)$  at large  $a$ .

The calculated binding energy values are not smooth near the energy minimum (Figure 1). This is due to our numerical errors. Binding energy does not change by more than 0.1% for  $\Delta a = 0.01$  [a.u.] near the energy minimum. We determined  $E_m$  from the fitting procedure since we found that they provide more accurate results. However, in most cases,  $E_m$  from our grid calculation and fitted  $E_m$  do not differ by more than 1%. We computed  $D_m$  and  $\tilde{D}_m$  using the atomic data we calculated numerically.

Our results for  $\text{H}_2^+$  and  $\text{H}_2$  are in good agreement with Turbiner & López Vieyra (2003) (hereafter TL03) and Lai & Salpeter (1996) (LS96) with less than 1% deviation in total binding energy (Tab. 1). TL03 performed highly accurate variational studies mainly on one-electron molecular systems (e.g.,  $\text{H}_2^+$ ,  $\text{H}_3^+$ ,  $\text{He}_2^{3+}$ ). LS96 studied hydrogen molecular structure similarly by a Hartree-Fock calculation in the adiabatic approximation. While our calculation takes into account higher Landau levels using perturbation theory, the difference

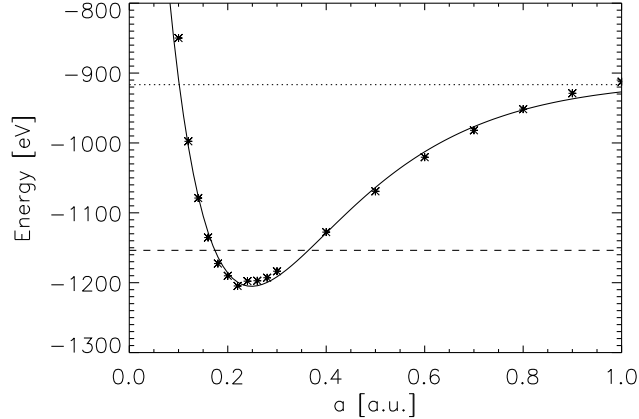


Fig. 1.— Binding energy curve of  $\text{He}_2$  at  $B = 10^{12}$  G. The solid curve is the fitted Morse function. The dashed line corresponds to the energy of two Helium atoms in the ground state  $(0, 1)$  ( $= -E_m + D_m$ ). The dotted line corresponds to the summed energy of one Helium atom in  $(0, 3)$  state and the other in  $(1, 2)$  state ( $= -E_m + \tilde{D}_m$ ).

in binding energies by including higher Landau levels is tiny for helium atoms and molecules at  $B \geq 10^{12}$  G.

Similar to hydrogen, the ground state configuration is  $(m_1, m_2) = (0, 1)$  for  $\text{He}_2^{2+}$  and  $(m_1, m_2, m_3, m_4) = (0, 1, 2, 3)$  for  $\text{He}_2$  at  $B \geq 10^{12}$  G. The accurate comparisons for helium molecules are Demeur et al. (1994) and ML06 who computed  $\text{He}_2$  binding energy by Hartree-Fock theory (table 2). Our results agree with ML06 within 1%. ML06 also computed helium molecular binding energies using density functional theory (ML06). However, their DFT results are less accurate than those of Hartree-Fock calculation; the binding energies are overestimated by  $\sim 10\%$  (ML06).

## 2.1. Electronic excitation

The electronic excited states in molecules occupy higher  $(m, \nu)$  states than those in atoms. Since excitation energies from the ground state to  $(0, 1, 2, m)$  states with  $m > 3$  are small, there may be numerous tightly-bound electronic excited states until they dissociate into atoms and ions at large  $m$ . We did not consider excited states with  $\nu > 0$  because their binding energies are small therefore they are likely to be dissociated. We calculated binding energies for the  $(0, 1, 2, m)$  state up to  $m = 9$  and estimated binding energies for higher  $m$  states using the well-known  $m$  dependence of the energy spacing  $\Delta E_m \sim \ln\left(\frac{2m+3}{2m+1}\right)$  (Lai et al. 1992). Figure 2 shows the  $\text{He}_2$  binding energy of  $(0, 1, 2, m)$  states at  $B = 10^{12}$

Table 1: Total binding energy [eV] of  $\text{H}_2^+$  (left) and  $\text{H}_2$  (right).

$B_{12}$	$m$	This work	LS96	TL03	$m_1, m_2$	This work	LS96
0.1	0	102	99.9	102	0, 1	162	161
1	0	233	232	233	0, 1	370	369
	1	162	162	162	0, 2	336	337
10	0	484	486	486	0, 1	772	769
	1	356	356	356	0, 2	713	709

---

Note. — LS96: Lai & Salpeter (1996), TL03: Turbiner & López Vieyra (2003)

Table 2: Total binding energy [eV] of  $\text{He}_2$  in comparison with ML06.

$B_{12}$	This work	ML06
1	1207	1202
10	2733	2728
100	5597	5598

G. Note that the excited states of  $\text{He}_2$ ,  $(0, 1, 2, m)$  with  $m > 5$ , are unbound with respect to two atoms in the ground state at  $B = 10^{12}$  G.

## 2.2. Aligned vibrational excitation

We fit the Morse function to molecular binding energies as a function of the nuclear separation  $a$ . Since we obtained  $E_m$ ,  $\tilde{D}_m$  and  $a_0$  from our numerical calculations,  $\beta$  is the only parameter which matters for the fit quality. Once  $\beta$  is determined, the aligned vibrational energy quanta is given by (LS96)

$$\hbar\omega_{\parallel} = \hbar\beta \left( \frac{2\tilde{D}_m}{\mu} \right)^{1/2} \quad (4)$$

where  $\mu$  is the reduced mass of the two nuclei in units of the electron mass (918 for  $\text{H}_2$  and 3675 for  $\text{He}_2$ ). At large  $a$ , another electron configuration is mixed with tightly-bound states (Lai et al. 1992). Since configuration interaction is neglected in our calculation, our

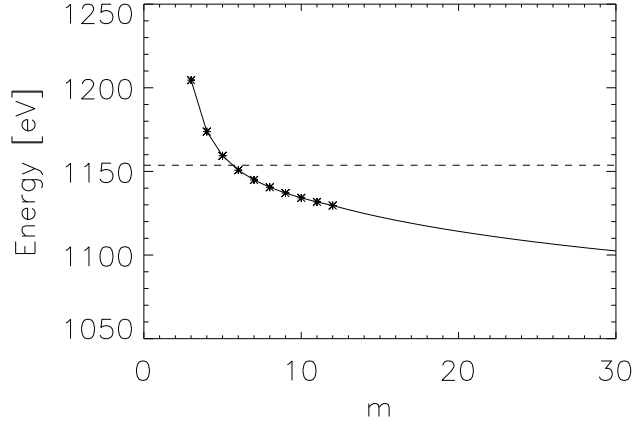


Fig. 2.— Binding energy curve of  $\text{He}_2$  in  $(0, 1, 2, m)$  states at  $B = 10^{12}$  G. The asterisk points are the binding energies from our numerical calculations. The dashed line corresponds to the energy of two Helium atoms in the ground state.

$\beta$  values (therefore  $\hbar\omega_{\parallel}$ ) are overestimated by 10–30% in comparison with LS96 (table 3). We found that  $\beta$  is nearly identical for different (tightly-bound) electronic excited states. Therefore we computed  $\hbar\omega_{\parallel}$  for electronic excited states with large  $m$  (for which we did not perform grid calculation) using  $\beta$  from the lower excited states. In most cases, our aligned vibrational energy quanta agree with other results within  $\sim 10\%$  (table 3). Table 4 shows aligned vibrational energy quanta for helium molecular ions.

Table 3: Aligned vibrational energy quanta  $\hbar\omega_{\parallel}$  [eV] of  $\text{H}_2^+$  (left) and  $\text{H}_2$  (right).

$B_{12}$	This work	LS96	TL03	This work	LS96
0.1	3.2	2.0	2.4	3.3	3.0
0.5	6.1	4.9	–	6.4	7.2
1	7.2	6.6	7.5	11	9.8
2	12	9.0	–	14	13
5	14	13	–	17	19
10	17	17	20	29	25

Table 4: Aligned vibrational energy quanta  $\hbar\omega_{\parallel}$  [eV] of helium molecular ions.

$B_{12}$	$\text{He}_2^{3+}$	$\text{He}_2^{2+}$	$\text{He}_2^+$	$\text{He}_2$
1	4.3	5.9	7.8	10
10	7.5	22	30	32
100	13	64	78	81

### 2.3. Transverse vibrational excitation

We calculated the energy curve as a function of transverse position of nuclei  $R$  following Ansatz A described in section IIIB of LS96. We fixed  $a$  to the equilibrium separation  $a_0$  and supposed that the two nuclei are located at  $(\pm R/2, \pm a_0/2)$ . As LS96 pointed out, this method is appropriate for small  $R$  ( $\lesssim \hat{\rho}$  where  $\hat{\rho}$  is the cyclotron radius) and gives only an upper limit to transverse vibrational energy quanta  $\hbar\omega_{\perp}$ . We replaced the nuclear Coulomb term in the Schrödinger equation  $V(z)$  by

$$V(z, R/2) = V_m\left(z - \frac{a_0}{2}, \frac{R}{2}\right) + V_m\left(z + \frac{a_0}{2}, \frac{R}{2}\right) \quad (5)$$

where

$$V_m(z, R/2) = \int d^2\vec{r}_{\perp} \frac{|\Phi_m(\vec{r}_{\perp})|^2}{|\vec{r}_{\perp} - \vec{R}/2|}. \quad (6)$$

We added  $\frac{Z^2 e^2}{(a_0^2 + R^2)^{1/2}}$  as the Coulomb repulsion energy between two nuclei. Once we calculated the molecular binding energy at different  $R$  grid points, we fit a parabolic form  $\frac{1}{2}\mu\omega_{\perp}^2 R^2$  to binding energies at  $R \lesssim \hat{\rho}$ . We found that  $\hbar\omega_{\perp}$  is nearly identical for different electronic excitation levels. Therefore, we adopted  $\hbar\omega_{\perp}$  of the ground state for electronic excited states. Our transverse vibrational energy quanta agree with those of LS96 and TL03 within 10% (table 5). Table 6 shows the results for helium molecular ions.

#### 2.3.1. Perturbative approach

It is also possible to estimate the transverse vibrational energy perturbatively, by calculating the lowest order perturbation to the energy of the molecule induced by tilting it. We assume that the energy of the tilted molecule is almost the same as the energy required to displacing the electron cloud relative to the molecule by an electric field ( $E$ ) :

$$\epsilon_{\kappa}^{(1)} = \langle \kappa | eEx | \kappa \rangle = 0. \quad (7)$$

Table 5: Transverse vibrational energy quanta  $\hbar\omega_{\perp}$  [eV] of  $\text{H}_2^+$  (left) and  $\text{H}_2$  (right). The numbers in the brackets are transverse vibrational energy [eV] computed using the perturbation theory.

$B_{12}$	This work	LS96	TL03	This work	LS96
0.1	2.8 (3.3)	3.1	2.9	2.5 (3.2)	2.6
0.5	8.7 (9.5)	9.8	–	8.7 (9.1)	8.7
1	14 (15)	16	15	14 (15)	14
2	22 (24)	25	–	22 (22)	23
5	42 (41)	45	–	41 (40)	42
10	63 (63)	70	66	64 (61)	65

Table 6: Transverse vibrational energy [eV]  $\hbar\omega_{\perp}$  of helium molecular ions. The numbers in the brackets are transverse vibrational energy [eV] computed using the perturbation theory.

$B_{12}$	$\text{He}_2^{3+}$	$\text{He}_2^{2+}$	$\text{He}_2^+$	$\text{He}_2$
1	9.8 (10)	10 (11)	9.7 (10)	10 (9.6)
10	46 (60)	50 (49)	48 (45)	50 (43)
100	205 (193)	216 (203)	217 (195)	216 (182)

The first-order change to the wavefunction is

$$\kappa^{(1)} = \sum_{\kappa'} \frac{\langle \kappa' | eEx | \kappa \rangle}{\epsilon_{\kappa'}^{(0)} - \epsilon_{\kappa}^{(0)}} \kappa' \quad (8)$$

where  $\epsilon_{\kappa}^{(0)}$  is the unperturbed energy of the state  $\kappa$  and  $\kappa'$  denotes the other states of the system.

The expectation value of  $x$  for this situation is

$$r \sin \theta = \langle x \rangle = eE \sum_{\kappa'} \frac{|\langle \kappa' | x | \kappa \rangle|^2}{\epsilon_{\kappa'}^{(0)} - \epsilon_{\kappa}^{(0)}} \quad (9)$$

where  $r$  is half the distance between the nuclei. We can solve for the value of  $eE$  that we need to apply to give a particular displacement and substitute it into the expression for the



energy of the state to second order

$$\epsilon_{\kappa}^{(2)} = (eE)^2 \sum_{\kappa'} \frac{|\langle \kappa' | x | \kappa \rangle|^2}{\epsilon_{\kappa'}^{(0)} - \epsilon_{\kappa}^{(0)}} = r^2 \sin^2 \theta \left( \sum_{\kappa'} \frac{|\langle \kappa' | x | \kappa \rangle|^2}{\epsilon_{\kappa'}^{(0)} - \epsilon_{\kappa}^{(0)}} \right)^{-1} \quad (10)$$

The only states that contribute to the sum have  $m' = m \pm 1$  for the electronic states of the molecule (the rotational states don't count because that is what we are examining). States that have been excited along the field ( $\nu > 0$ ) or by increasing the Landau number do not have much overlap in the integral in the numerator and also a large energy difference in the denominator.

The frequency for low amplitude oscillations is given by

$$\omega_{\perp}^2 = \frac{2r^2}{I} \left( \sum_{\kappa'} \frac{|\langle \kappa' | x | \kappa \rangle|^2}{\epsilon_{\kappa'}^{(0)} - \epsilon_{\kappa}^{(0)}} \right)^{-1} = \frac{1}{M} \left( \sum_{\kappa'} \frac{|\langle \kappa' | x | \kappa \rangle|^2}{\epsilon_{\kappa'}^{(0)} - \epsilon_{\kappa}^{(0)}} \right)^{-1} \quad (11)$$

where  $I$  is the moment of inertia of the molecule,  $2Mr^2$  ( $M$  is the nuclear mass). The size of the molecule has cancelled out.

For a single electron system in the ground state if we assume that the bulk of the contribution to the sum in the equation is given by the  $m = 1, \nu = 0$  state we have

$$\omega_{\perp} \approx \frac{\sqrt{2}}{\hat{\rho}} \left( \frac{\epsilon_{m=1, \nu=0} - \epsilon_{m=0, \nu=0}}{M} \right)^{1/2} |\langle f_{m=1, \nu=0} | f_{m=0, \nu=0} \rangle| \quad (12)$$

where the final term is the overlap of the longitudinal wavefunction of the two states.

For a multielectron system, evaluating equation (10) and (11) is somewhat more complicated. For clarity of nomenclature we shall write the wavefunctions of the various electronic states of the molecule as  $\mathcal{K}'$ . The symbol  $\mathcal{K}$  denotes the state that we are focused upon. The change in the energy of the system due to an applied electric field is

$$\epsilon^{(1)} = \langle \mathcal{K} | NeE\bar{x} | \mathcal{K} \rangle = 0 \quad (13)$$

where  $N$  is the number of electrons and

$$N\bar{x} = \sum_j x_j \quad (14)$$

where  $j$  counts over the electrons in the molecule. We have assumed that the multielectron wavefunctions are normalized such that  $\langle \mathcal{K} | \mathcal{K} \rangle = 1$

The first-order change to the wavefunction is

$$\mathcal{K}^{(1)} = \sum_{\mathcal{K}'} \frac{\langle \mathcal{K}' | NeE\bar{x} | \mathcal{K} \rangle}{\epsilon_{\mathcal{K}'}^{(0)} - \epsilon_{\mathcal{K}}^{(0)}} \mathcal{K}' \quad (15)$$

where  $\epsilon_{\mathcal{K}'}^{(0)}$  is the unperturbed energy of the state  $\mathcal{K}'$ .

Now let's calculate the expectation value of  $\bar{x}$  for this situation,

$$r \sin \theta = \langle \bar{x} \rangle = NeE \sum_{\mathcal{K}'} \frac{|\langle \mathcal{K}' | \bar{x} | \mathcal{K} \rangle|^2}{\epsilon_{\mathcal{K}'}^{(0)} - \epsilon_{\mathcal{K}}^{(0)}} \quad (16)$$

where  $r$  is half the distance between the nuclei. We can solve for the value of  $NeE$  that we need to apply to give a particular displacement and substitute it into the expression for the energy of the state to second order

$$\epsilon_{\mathcal{K}}^{(2)} = (NeE)^2 \sum_{\mathcal{K}'} \frac{|\langle \mathcal{K}' | \bar{x} | \mathcal{K} \rangle|^2}{\epsilon_{\mathcal{K}'}^{(0)} - \epsilon_{\mathcal{K}}^{(0)}} = r^2 \sin^2 \theta \left( \sum_{\mathcal{K}'} \frac{|\langle \mathcal{K}' | \bar{x} | \mathcal{K} \rangle|^2}{\epsilon_{\mathcal{K}'}^{(0)} - \epsilon_{\mathcal{K}}^{(0)}} \right)^{-1} \quad (17)$$

In strongly magnetized atoms or molecules, it is natural to expand the wavefunctions in terms of the ground Landau level using various values of  $m$ . Let's assume that the wavefunction for each electron is written as

$$\kappa_j = \frac{1}{\sqrt{2\pi}} \Phi_{m_j}(\rho) f_j(z) e^{im_j \phi}. \quad (18)$$

In this case we have

$$\langle \kappa_i | x | \kappa_j \rangle = \frac{\hat{\rho}}{2} \sqrt{2(m_j + 1)} \langle f_i | f_j \rangle \text{ if } m_i = m_j + 1 \quad (19)$$

otherwise it vanishes.

Combining these results yields an estimate for the frequency of low amplitude oscillations of

$$\omega_{\perp} \approx \frac{N\sqrt{2}}{\hat{\rho}} \left( \frac{\epsilon_{m+1} - \epsilon_m}{M(m+1)} \right)^{1/2} |\langle f_i | f \rangle| \quad (20)$$

where the subscript on energy labels the value of  $m$  in the outermost shell. The number of electrons appears in this equation because the expectation value of  $\bar{x}$  is a factor  $N$  smaller than the expectation value of  $x$  for the single shifted electron.

For the ground state of the molecule we have  $m+1 = N$  yielding a simpler expression,

$$\omega_{\perp} \approx \frac{\sqrt{2}}{\hat{\rho}} \left( N \frac{\epsilon_{m+1} - \epsilon_m}{M} \right)^{1/2} |\langle f_i | f \rangle|. \quad (21)$$

Table 5 and 6 compare the perturbative estimates with the numerical calculations. Within the approximations made the agreement is encouraging.

### 3. Rotovibrational spectrum

Given the aligned and transverse vibrational energies, we construct the rotovibrational spectra of helium molecules. Strictly speaking, the aligned and transverse vibrations are coupled (Khersonskii 1984; Lai & Salpeter 1996). However, using perturbation theory, Khersonskii (1985) has shown that the coupling energy is tiny (less than 1%) compared to the total binding energy. Neglecting the coupling, the rotovibrational energy levels are well approximated by

$$\epsilon_{NAV} = \epsilon_V + \epsilon_{N\Lambda} \quad (22)$$

$$\epsilon_{N\Lambda} = \hbar\omega_t \left( N + \frac{|\Lambda| + 1}{2} \right) - \frac{\Lambda}{2} \hbar\omega_B \quad (23)$$

$$\epsilon_V = \hbar\omega_{\parallel} \left( V + \frac{1}{2} \right) - \frac{(\hbar\omega_{\parallel})^2}{4\tilde{D}_m} \left( V + \frac{1}{2} \right)^2 \quad (24)$$

where  $\hbar\Omega_B$  is the nuclear cyclotron energy ( $= Z\hbar eB/(Am_p c) = 6.3(Z/A)B_{12}$  [eV] where  $Z$  is the nuclear charge and  $A$  is the atomic mass) and  $\omega_t = \sqrt{4\omega_{\perp}^2 + \Omega_B^2}$ . The nuclear cyclotron energy term takes into account the magnetic restoring force on the helium nuclei (Lai & Salpeter 1996). The integer  $N$  is the quantum number for the transverse vibration, while the integer  $V$  is the quantum number for the aligned vibration.  $\Lambda$  is the projection of angular momentum in the B-field direction. Molecular states with  $\epsilon_{NAV} > D_m$  will dissociate to atoms and ions. From the above equations, the molecular system has a finite zero-point energy associated with aligned and transverse vibration

$$\epsilon_{000} = \frac{1}{2}(\hbar\omega_t + \hbar\omega_{\parallel}) \quad (25)$$

when  $N = \Lambda = V = 0$ . Therefore, the actual dissociation energy will be reduced from  $D_m$  by  $\epsilon_{000}$  (LS96). Figure 3 shows the rotovibrational energy spectrum of  $\text{He}_2$  in the ground state at  $B = 10^{12}$  G and  $10^{13}$  G respectively. Table 7 shows the number of rotovibrational states of various helium molecular ions. The number of rotovibrational states decreases for higher electronic excited states. The magnetic field dependence is more complicated due to the following reasons. The number of aligned vibrational levels generally increases with  $B$ . On the other hand, the number of transverse vibrational ( $N$ ) and rotational ( $\Lambda$ ) levels increases with  $B$  at  $B < B_Q$  while it decreases with  $B$  at  $B > B_Q$ . This is because the ion cyclotron energy ( $\propto B$ ) dominates over  $\hbar\omega_{\perp}$  ( $\propto B^{1/2}$ ) at  $B > B_Q$ . It should be noted that only those rotovibrational states with excitation energies that are smaller than or similar to the thermal energy have large statistical weights in the partition function (§5).

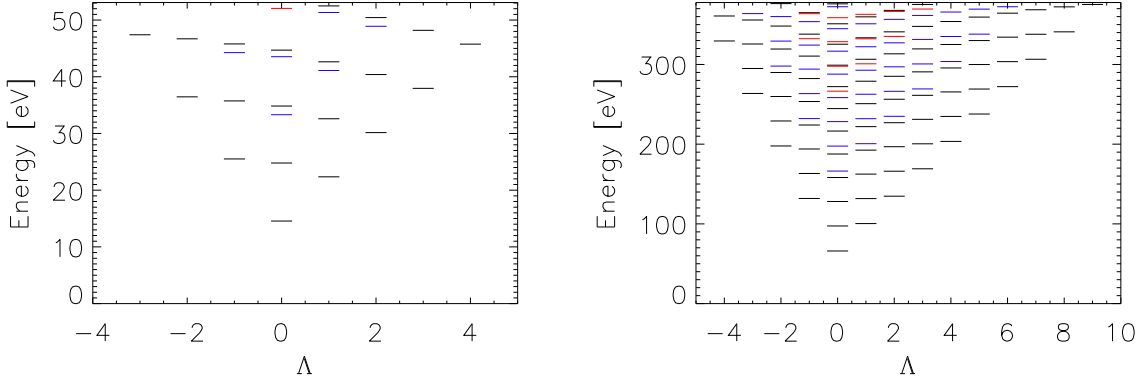


Fig. 3.— Rotovibrational energy spectrum ( $\epsilon_{NAV}$ ) of  $\text{He}_2$  in the ground state at  $B = 10^{12}$  G (left) and  $10^{13}$  G (right). The zero energy corresponds to  $E = -E_m$ , while the uppermost horizontal line corresponds to  $E = -E_m + D_m$  above which the molecular states become dissociated. The black, blue and red lines indicate  $N = 0, 1$  and  $2$  state. For each  $N$  and  $\Lambda$ , the horizontal lines indicate energy levels for different  $V$  states.

#### 4. Effects of finite nuclear mass

So far, we have assumed that the nuclear mass is infinite. The separation of the center-of-mass motion is non-trivial when a magnetic field is present. There are two effects that modify the energy levels from the infinite nuclear mass case. We denote the binding energy in the infinite nuclear mass approximation as  $\epsilon_\kappa^{(0)} (< 0)$  for an electronic state  $\kappa$ . Since we consider states with  $n = 0$  and  $\nu = 0$ , the relevant quantum numbers are  $\kappa = \{m_i\}$  ( $i$  denotes each bound electron in multi-electron atoms and molecules).

##### 4.1. Finite nuclear mass correction

The conservation of the total pseudomomentum ( $\vec{K}$ ) introduces an additional term  $s_\kappa \hbar \Omega_B$  in the binding energy (Herold et al. 1981).  $\Omega_B$  is the nuclear cyclotron energy and  $s_\kappa = \sum_i m_i$  is the sum of magnetic quantum numbers for a given electronic state  $\kappa$  (e.g.,  $s_\kappa = 4$  for  $\text{He}_2$  molecule in the ground state). However, this scheme does not necessarily give the lowest binding energies at  $B > B_Q$ . Instead, LS95 and LS96 estimated lower binding energies at  $B > B_Q$  using another scheme which relaxed the assumption of the zero transverse pseudomomentum. A more rigorous calculation was performed for  $\text{He}^+$  ion by Bezchastnov et al. (1998) and Pavlov & Bezchastnov (2005). An application of such schemes to multi-electron systems is beyond the scope of this paper. We will discuss the limitation of our models at very high magnetic field in §5.

Table 7: Number of rovibrational states in helium molecular ions.

	$(m_1, m_2, m_3, m_4)$	$B_{12} = 1$	$B_{12} = 10$	$B_{12} = 100$
$\text{He}_2^{3+}$	(0)	0	0	1
$\text{He}_2^{2+}$	(0,1)	0	8	12
	(0,2)	0	0	1
$\text{He}_2^+$	(0,1,2)	98	177	87
	(0,1,3)	5	79	56
	(0,1,4)	0	46	42
	(0,1,5)	0	31	35
$\text{He}_2$	(0,1,2,3)	27	132	87
	(0,1,2,4)	2	77	61
	(0,1,2,5)	0	57	52
	(0,1,2,6)	0	50	46

#### 4.2. Motional Stark effects

When an atom or molecule moves across the magnetic field  $\vec{B}$ , a motional Stark electric field  $\vec{E}_{MS} = \frac{\vec{K} \times \vec{B}}{Mc}$  is induced in the center-of-mass frame.  $M$  is the mass of atom or molecule. The Hamiltonian for the motional Stark field is given by

$$H_{MS} = e \frac{\vec{K} \times \vec{B}}{Mc} \vec{r} = \Omega_{B0} K_{\perp} x \quad (26)$$

where  $\Omega_{B0} \equiv \frac{eB}{Mc}$ . For a given pseudomomentum  $\vec{K}$ , the motional Stark field separates the guiding center of the nucleus and that of the electron by

$$R_K = \frac{c|\vec{K} \times \vec{B}|}{eB^2} = \frac{cK_{\perp}}{eB}. \quad (27)$$

Since the motional Stark field breaks the cylindrical symmetry preserved in magnetic field, it is non-trivial to evaluate motional Stark field effects. A non-perturbative (therefore more rigorous) approach has been applied only for one-electron systems (Vincke et al. 1992; Potekhin 1994; Pavlov & Bezchastnov 2005). However, such an approach is quite complicated and time-consuming especially for multi-electron atoms and molecules. Therefore, following LS95, we considered two limiting cases: (1)  $R_K \ll \hat{\rho}$  and (2)  $R_K \gg \hat{\rho}$  and determined general formula which can be applied to a wide range of  $B$  and  $K_{\perp}$ . For diatomic molecules, we can apply a nearly identical scheme used for calculating transverse vibrational energy to the both cases.

#### 4.2.1. Centered states

When the energy shift caused by motional Stark field is smaller than the spacing between binding energies, the perturbation approach is applicable (Pavlov & Meszaros (1993) and § 2.3.1). The first order perturbation energy  $\langle \kappa | H_{MS} | \kappa \rangle$  vanishes since the matrix element  $\langle \kappa | x | \kappa \rangle = 0$ . The second order perturbation energy is given by

$$\epsilon_{\kappa}^{(2)} = \sum_{\kappa'} \frac{|\langle \kappa' | H_{MS} | \kappa \rangle|^2}{\epsilon_{\kappa'}^{(0)} - \epsilon_{\kappa}^{(0)}} = \frac{K_{\perp}^2}{2M} \alpha_{\kappa}^{(2)} \quad (28)$$

Among the various electronic states  $\kappa' = \{n' m' \nu'\}$ , only  $n' = 0, m' = m \pm 1, \nu' = 0$  state have non-negligible contribution to  $\epsilon_{\kappa}^{(2)}$  since the other states have large  $\epsilon_{\kappa'}^{(0)} - \epsilon_{\kappa}^{(0)}$  and/or vanishing matrix element  $\langle \kappa' | x | \kappa \rangle$ . Since the overlap integral of longitudinal wavefunction is close to unity (Pavlov & Meszaros 1993),  $\alpha_{\kappa}^{(2)}$  is given by

$$\alpha_{\kappa}^{(2)} \simeq \hbar \Omega_{B0} \left( \frac{m+1}{\epsilon_m - \epsilon_{m+1} + \hbar \Omega_{Bi}} + \frac{m}{\epsilon_m - \epsilon_{m-1} - \hbar \Omega_{Bi}} \right) \quad (29)$$

where  $\epsilon_m = -\epsilon_{\kappa}^{(0)} (> 0)$  where  $m$  denotes the magnetic quantum number of the outermost electron of electronic state  $\kappa$ . The 2nd term is zero for the ground state. Following Pavlov & Meszaros (1993), we define the anisotropic mass  $M_{\perp, \kappa}$  as

$$M_{\perp, \kappa} \equiv \frac{M}{1 - \alpha_{\kappa}^{(2)}} > M. \quad (30)$$

The transverse energy characterized by  $K_{\perp}$  is given by

$$E_{\perp, \kappa} = \frac{K_{\perp}^2}{2M_{\perp, \kappa}}. \quad (31)$$

The perturbation method is valid when  $|\epsilon_{\kappa}^{(2)}| \ll |\Delta \epsilon_{\kappa}^{(0)}|$  (Pavlov & Meszaros 1993) where  $K_{\perp, \kappa}$  is given by

$$K_{\perp, \kappa} = \left( \frac{2M |\Delta \epsilon_{\kappa}^{(0)}|}{\alpha_{\kappa}^{(2)}} \right)^{1/2}. \quad (32)$$

where  $|\Delta \epsilon_{\kappa}^{(0)}|$  is the spacing of the zeroth order energies (typically  $|\epsilon_m - \epsilon_{m+1}|$ ).

#### 4.2.2. Decentered states

When  $R_K \gg \hat{\rho}$ , it is convenient to utilize the so-called decentered formalism (LS95). We replace the nuclear Coulomb term by

$$V_m(z, R_K) = \int d^2 \vec{r}_{\perp} \frac{|\Phi_m(\vec{r}_{\perp})|^2}{|\vec{r}_{\perp} + \vec{R}_K|}, \quad (33)$$

and compute binding energies at different  $R_K$  grid points. For diatomic molecules, we replace the nuclear Coulomb term by

$$V(z, R_K) = V_m\left(z - \frac{a_0}{2}, R_K\right) + V_m\left(z + \frac{a_0}{2}, R_K\right). \quad (34)$$

The grid calculation for  $R_K$  is identical to the one for transverse vibrational energy in §2.3 except that the Coulomb repulsion term between two nuclei is  $\frac{Z^2 e^2}{a_0}$  (instead of  $\frac{Z^2 e^2}{(a_0^2 + R_K^2)^{1/2}}$ ) since motional Stark field shifts the guiding center of the two nuclei by  $R_K$  in the transverse direction but the separation between the two nuclei is still  $a_0$ .

LS95 found that the binding energy curves are well fit by the following formula.

$$E_\perp(K_\perp) + \epsilon_\kappa^{(0)} = -A_1 \left( \ln \frac{1}{A_2 + A_3 R_K^2} \right)^2 \quad (35)$$

where  $A_1, A_2$  and  $A_3$  are the fit parameters.  $E_\perp(R_K) = E_\perp(K_\perp)$  is the transverse energy and  $\epsilon_\kappa^{(0)}$  is the binding energy in the infinite nuclear mass approximation. Figure 4 shows the binding energy curve of  $\text{He}_2$  molecule as a function of  $R_K$  at  $B = 10^{12}$  G. At small  $R_K$ , the fitted function is well matched with the results from the perturbation approach. Although mixing between different  $m$  states is ignored, a comparison with Potekhin (1998) and Potekhin (1994) for hydrogen atoms indicates this approach gives better than 30% accuracy over a large range of  $K_\perp$  (Lai & Salpeter 1995). This is adequate for our purpose of investigating ionization and dissociation balance.

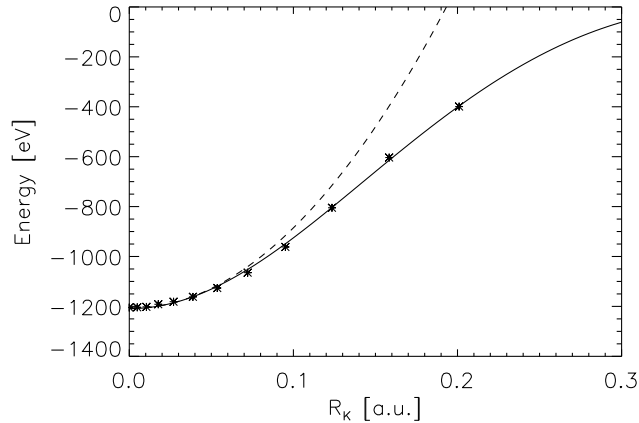


Fig. 4.— The transverse energy of  $\text{He}_2$  molecule at  $B = 10^{12}$  G. The asterisks are the binding energies from our numerical calculation and they are fitted with the function given in (35). The dashed line shows the energy curve from the perturbation method discussed in §2.3.1 and §4.2.1.

Along with the finite nuclear mass term discussed in §4.1, the electronic energy of an atom or molecule moving with transverse pseudomomentum  $K_\perp$  is given by

$$\epsilon_\kappa(K_\perp) = \epsilon_\kappa^{(0)} + s_\kappa \hbar \Omega_B + E_\perp(K_\perp). \quad (36)$$

Note that  $\epsilon_\kappa^{(0)} < 0$  and both the second and third term decrease the binding energy. Later, we will discuss the validity of this approach at  $B \gg B_Q$ .

## 5. Ionization and dissociation equilibrium

We have investigated the ionization and dissociation balance of magnetized helium atmospheres including the following chemical reaction channels. Table 8 and 9 list ionization and dissociation energies of various helium ions and molecular ions in the infinite nuclear mass assumption. We did not take into account the  $\text{He}^-$  ion since its ionization energy is  $\lesssim 20$  [eV] and  $\text{He}^-$  is not abundant at all in the temperature range considered here ( $T \gtrsim 10^5$  K).

- Ionization

- (1)  $\text{He}^+ \leftrightarrow \alpha + \text{e}$
- (2)  $\text{He} \leftrightarrow \text{He}^+ + \text{e}$
- (3)  $\text{He}_2^{2+} \leftrightarrow \text{He}_2^{3+} + \text{e}$
- (4)  $\text{He}_2^+ \leftrightarrow \text{He}_2^{2+} + \text{e}$
- (5)  $\text{He}_2 \leftrightarrow \text{He}_2^+ + \text{e}$

- Dissociation

- (6)  $\text{He}_2^{3+} \leftrightarrow \alpha + \text{He}^+$
- (7)  $\text{He}_2^{2+} \leftrightarrow \alpha + \text{He}$
- (8)  $\text{He}_2^{2+} \leftrightarrow \text{He}^+ + \text{He}^+$
- (9)  $\text{He}_2^+ \leftrightarrow \text{He}^+ + \text{He}$
- (10)  $\text{He}_2 \leftrightarrow \text{He} + \text{He}$

The Saha-Boltzmann equation for ionization balance is given as,

$$\frac{n_i}{n_{i+1}n_e} = \frac{z_i}{z_{i+1}z_e} \quad (37)$$



Table 8: Ionization energy [eV] of helium atom and molecular ions.

$B_{12}$	$\text{He}^+$	$\text{He}$	$\text{He}_2^{3+}$	$\text{He}_2^{2+}$	$\text{He}_2^+$	$\text{He}_2$
1	418	159	391	418	261	137
10	847	331	885	947	603	298
100	1563	629	1833	1912	1209	643

Table 9: Dissociation energy  $D_m$  [eV] of helium molecular ions. The numbers in the brackets are  $\tilde{D}_m$  [eV]. The columns without a number indicate that there is no bound molecular state with respect to ions and atoms. The zero-point energy correction is not included.

$B_{12}$	$\text{He}_2^{3+}$	$\text{He}_2^{2+}$	$\text{He}_2^+$	$\text{He}_2$
1	– (–)	– (97.8)	74.6 (251)	53.1 (290)
10	37.8 (37.8)	137 (359)	410 (725)	378 (806)
100	270 (270)	619 (973)	1198 (1708)	1212 (1915)

where  $z_e$  is the partition function for an electron,

$$z_e = 2 \left( \frac{m_e kT}{2\pi\hbar^2} \right)^{3/2} \frac{\eta_e}{\tanh \eta_e}, \quad (38)$$

$\eta_e = \hbar\omega_B/2kT$  and  $\omega_B = eB/m_e c$  is the electron cyclotron frequency (Lai 2001). The quantity  $z_i$  is the partition function for ionization state  $i$ ,

$$z_i = \left( \frac{M_i kT}{2\pi\hbar^2} \right)^{1/2} \frac{\eta_i}{\sinh \eta_i} \int_0^\infty \frac{K_\perp dK_\perp}{2\pi\hbar^2} \sum_\kappa w_{i,\kappa}(K_\perp) \exp \left( -\frac{\epsilon_{i,\kappa}(K_\perp)}{kT} \right) \quad (39)$$

where  $E_i$ ,  $Z_i$  and  $M_i$  are the ground state energy, the charge and the mass of an ion  $i$ .  $\eta_i = \hbar\Omega_{Bi}/2kT$  where  $\Omega_{Bi} = Z_i eB/M_i c$  is the ion cyclotron frequency.  $\epsilon_{i,\kappa}(K_\perp) (< 0)$  is the binding energy of a bound state  $\kappa$  given in equation (36).  $w_{i,\kappa}$  is the occupation probability. In general,  $w_{i,\kappa}(K_\perp)$  is a function of  $Z_i$ ,  $Z_p$  (the charge of perturbing ions, usually the effective charge of the plasma),  $\epsilon_{i,\kappa}(K_\perp)$  and  $\rho$  (the plasma density).  $w$  depends not only on the type of ion  $i$ , the electronic state  $\kappa$  and the transverse pseudomomentum  $K_\perp$ , but also it is different for each bound electron. Obviously, electrons in the outer shells are subject to a stronger electric field from neighboring ions than those in the inner shells. We explicitly computed  $w_{i,\kappa}$  for all the bound electrons using the electronic microfield distribution of Potekhin et al. (2002).

The Saha-Boltzmann equation for dissociation balance is given as

$$\frac{n_j}{n_k n_l} = \frac{\tilde{z}_j}{z_k z_l} \quad (40)$$

where  $\tilde{z}_j$  is the partition function for molecular ionization state  $j$ ,

$$\tilde{z}_j = \left( \frac{M_j kT}{2\pi\hbar^2} \right)^{1/2} \frac{\eta_j}{\sinh \eta_j} \int_0^\infty \frac{K_\perp dK_\perp}{2\pi\hbar^2} \sum_\kappa w_{j,\kappa}(K_\perp) \exp\left(-\frac{\epsilon_{j,\kappa}(K_\perp)}{kT}\right) \sum_{N,\Lambda,V}^{\epsilon_{NAV} < D_\kappa} \exp\left(-\frac{\epsilon_{NAV}}{kT}\right) \quad (41)$$

where  $E_j$ ,  $Z_j$  and  $M_j$  are the ground state energy, the charge and the mass of a molecular ion  $j$ .  $\eta_j = \hbar\Omega_{Bj}/2kT$  where  $\Omega_{Bj} = Z_j eB/M_j c$  is the molecular ion cyclotron frequency.  $\epsilon_{j,\kappa}(K_\perp) (< 0)$  and  $w_{j,\kappa}(K_\perp)$  are the binding energy and occupation probability of an electronic bound state  $\kappa$ .  $\epsilon_{NAM} (> 0)$  is the excitation energy of a rotovibrational state  $(N, \Lambda, V)$ . We took the summation  $\sum_{N,\Lambda,V}$  until  $\epsilon_{NAV}$  exceeds the dissociation energy  $D_\kappa$ . The set of the Saha-Boltzmann equations along with the condition for the baryon number conservation and charge neutrality are iteratively solved until we reached sufficient convergence in  $\Delta n_e/n_e$  ( $< 10^{-6}$ ) where  $n_e$  is the density of free electrons. The convergence was achieved rapidly in most cases (less than 10 iterations were required).

Figure 5, 6 and 7 show the fraction of helium ions and molecular ions at  $B = 10^{12}, 10^{13}$  and  $10^{14}$  G. At  $B = 10^{12}$  G,  $\text{He}_2^{3+}$  and  $\text{He}_2^{2+}$  are not present because they are not bound with respect to their dissociated atoms and ions (table 9). In all the cases, the  $\text{He}_2^{3+}$  fraction is negligible because helium molecular ions with more electrons have much larger binding energies. At  $B = 10^{14}$  G,  $\text{He}_2$  is not present because even the ground state becomes auto-ionized to  $\text{He}_2^+$  ion due to the finite nuclear mass effect although  $\text{He}_2$  remains bound with respect to two helium atoms. Note that the ionization energy of  $\text{He}_2$  at  $10^{14}$  G is 643 eV (table 8) while the difference in the energy due to the finite nuclear mass term between  $\text{He}_2$  and  $\text{He}_2^+$  is 945 eV. As discussed in §4.1, our scheme becomes invalid at  $B > B_Q$  and in reality  $\text{He}_2$  will have lower binding energy than  $\text{He}_2^+$ . Therefore, our results at  $B = 10^{14}$  G should be taken with caution. Figure 8 shows the temperature dependence of the helium atomic and molecular fractions at different B-field strengths. We fixed the plasma density to the typical density of the X-mode photosphere ( $\sim 10, 10^2$  and  $10^3$  g/cm<sup>3</sup> for  $B = 10^{12}, 10^{13}$  and  $10^{14}$  G (Lai & Salpeter 1997)). The transition from molecules to helium atoms and ions takes place rapidly at  $T \sim 3 \times 10^5$  K and  $\sim 6 \times 10^5$  K for  $B = 10^{12}$  G and  $10^{13}$  G.

In order to illustrate different physical effects, we show the fraction of helium atoms and  $\text{He}_2$  molecules as a function of temperature in Figure 9. When motional Stark effects are ignored (dotted line), the molecular fraction is underestimated because helium ions and atoms are subject to a larger motional Stark field due to their smaller masses and binding energies. As expected, molecules become more abundant when rotovibrational states are

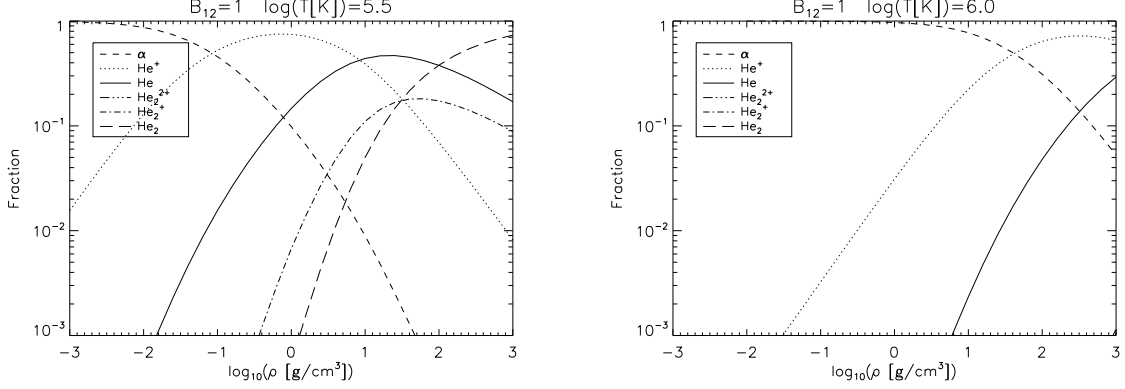


Fig. 5.— Ionization and dissociation balance of helium at  $T = 10^{5.5}$  K (left) and  $10^6$  K (right) at  $B = 10^{12}$  G.

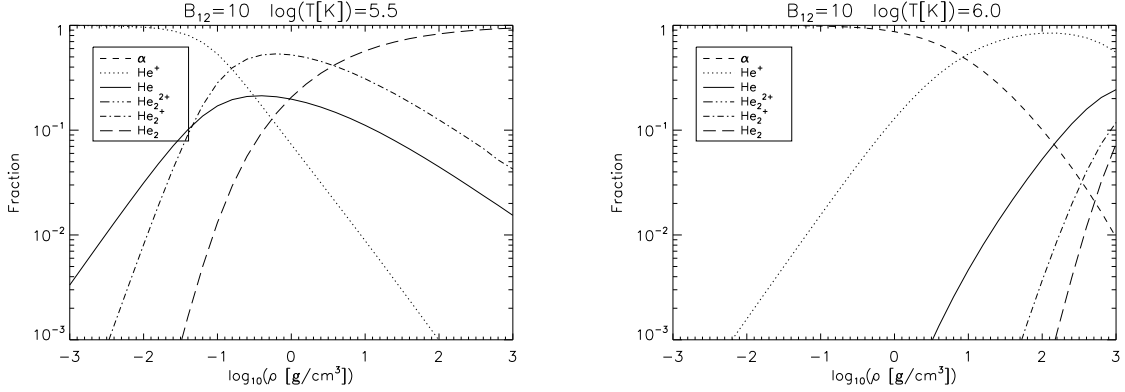


Fig. 6.— Ionization and dissociation balance of helium at  $T = 10^{5.5}$  K (left) and  $T = 10^6$  K (right) at  $B = 10^{13}$  G.

included. The discrepancy from the results without rovibrational states (dashed line) increases toward higher temperature since more rovibrational states have larger statistical weight as their excitation energies are an order of 100 eV at  $B = 10^{13}$  G (see figure 3). When we take into account only the ground states (dot-dashed line), the results are close to the case without motional Stark effects because the ground states are less affected by motional Stark effects than the excited states.

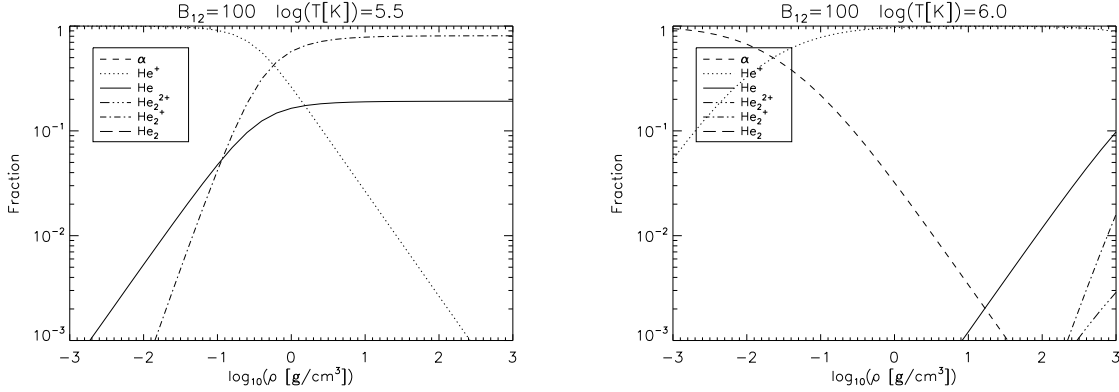


Fig. 7.— Ionization and dissociation balance of helium at  $T = 10^{5.5}$  K (left) and  $T = 10^6$  K (right) at  $B = 10^{14}$  G.

### 5.1. $\text{He}_3$ molecule and larger helium molecular chains

When  $\text{He}_2$  is abundant, larger helium molecules such as  $\text{He}_3$  may become abundant. We roughly estimated the fraction of  $\text{He}_3$  molecules by neglecting the finite nuclear mass effects and zero-point vibrational energy correction both of which will reduce the dissociation energy. Similarly to  $\text{He}_2$ , we computed the binding energy of  $\text{He}_3$  molecules by Hartree-Fock calculation. The dissociation energy of  $\text{He}_3 \rightarrow \text{He}_2 + \text{He}$  is 289 and 1458 eV at  $B = 10^{13}$  and  $10^{14}$  G. Our results are close to those of the density functional calculation by ML06 (384 and 1647 [eV] at  $B = 10^{13}$  and  $10^{14}$  G). Note that the density function calculation overestimates binding energies by  $\sim 10\%$  compared with more accurate Hartree-Fock calculation (ML06). Assuming the internal degrees of freedom are similar between  $\text{He}_2$  and  $\text{He}_3$  molecule and neglecting the bending degree of freedom for  $\text{He}_3$ , we computed dissociation equilibrium between  $\text{He}_2$  and  $\text{He}_3$  following Lai & Salpeter (1997).

Figure 10 shows contours of the  $\text{He}_3$  molecule fraction with respect to  $\text{He}_2$  molecule at  $B = 10^{13}$  G. In the dotted area, the fraction of diatomic helium molecular ions is larger than 10%. It is seen that  $\text{He}_3$  molecule will be abundant at  $T \lesssim 3 \times 10^5$  K at  $B = 10^{13}$  G. The results are consistent with the estimates of molecular chain formation by Lai (2001) and ML06. ML06 provided binding energy of infinite He molecular chain as  $E_\infty \simeq 1.25 B_{13}^{0.38}$  keV at  $B \gtrsim 10^{13}$  G. From this fitting formula, the cohesive energy of helium molecular chains is given as  $E_{co} \sim 0.36, 1.5$  and  $5.1$  keV at  $B = 10^{13}, 10^{14}$  and  $10^{15}$  G. When  $kT \lesssim 0.1 E_{co}$ , molecular chains are likely to be formed (Lai 2001); consequently, we expect helium molecular chains to form at  $T \lesssim 3 \times 10^5, 1 \times 10^6$  and  $5 \times 10^6$  K and  $B \gtrsim 10^{13}, 10^{14}$  and  $10^{15}$  G.

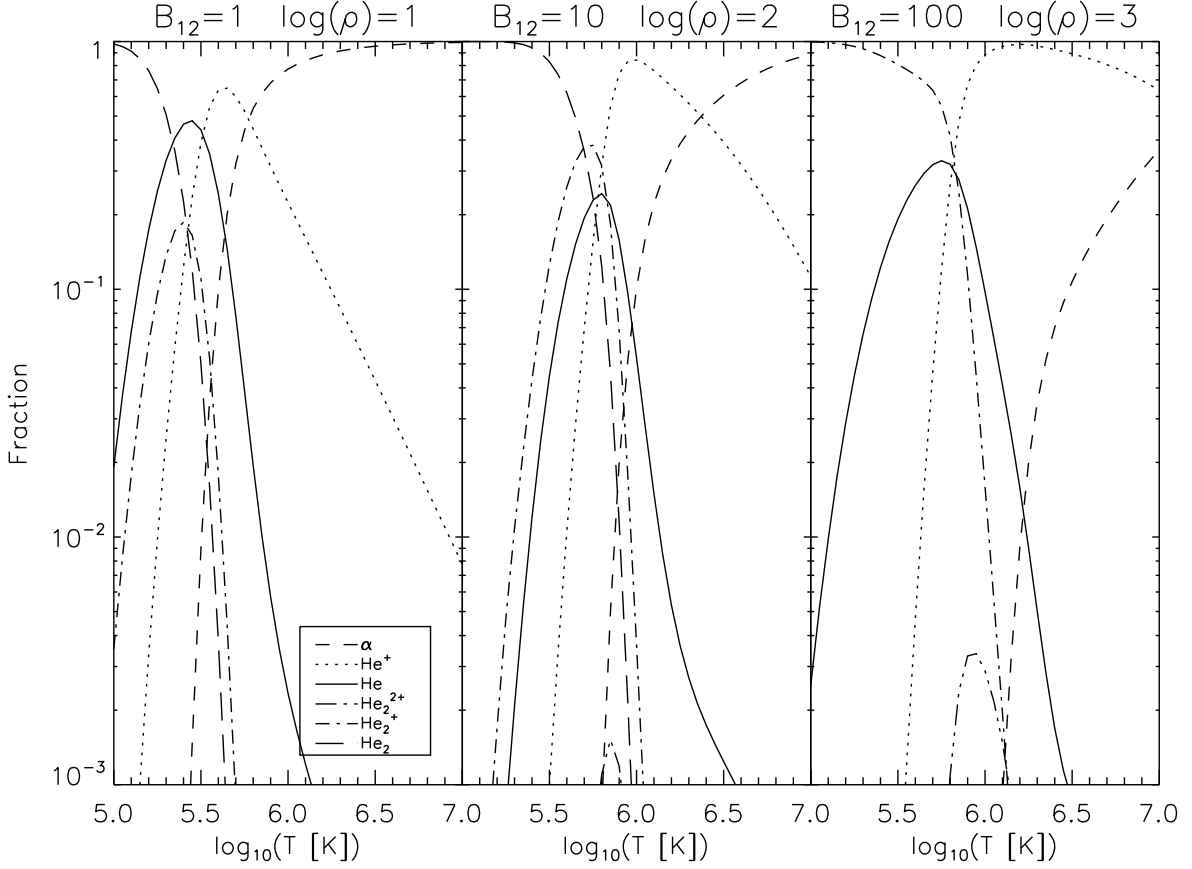


Fig. 8.— Temperature dependence of helium atomic and molecular fraction at  $B = 10^{12}$  G ( $\rho = 10$  g/cm<sup>3</sup>),  $B = 10^{13}$  G ( $\rho = 10^2$  g/cm<sup>3</sup>) and  $B = 10^{14}$  G ( $\rho = 10^3$  g/cm<sup>3</sup>).

## 6. Application

We investigated the ionization and dissociation balance of helium atmospheres for two classes of INS whose X-ray spectra show absorption features.

### 6.1. Radio-quiet neutron stars

A class of INS called radio-quiet neutron stars (RQNS) is characterized by their X-ray thermal spectra with  $T \lesssim 10^6$  K and spin-down dipole B-field strength  $B \gtrsim 10^{13}$  G. A single or multiple absorption features have been detected from six radio-quiet NS (Haberl et al. 2003, 2004; van Kerkwijk et al. 2004). Although the interpretation of these features is still in debate, helium is certainly one of the candidates for the surface composition of RQNS

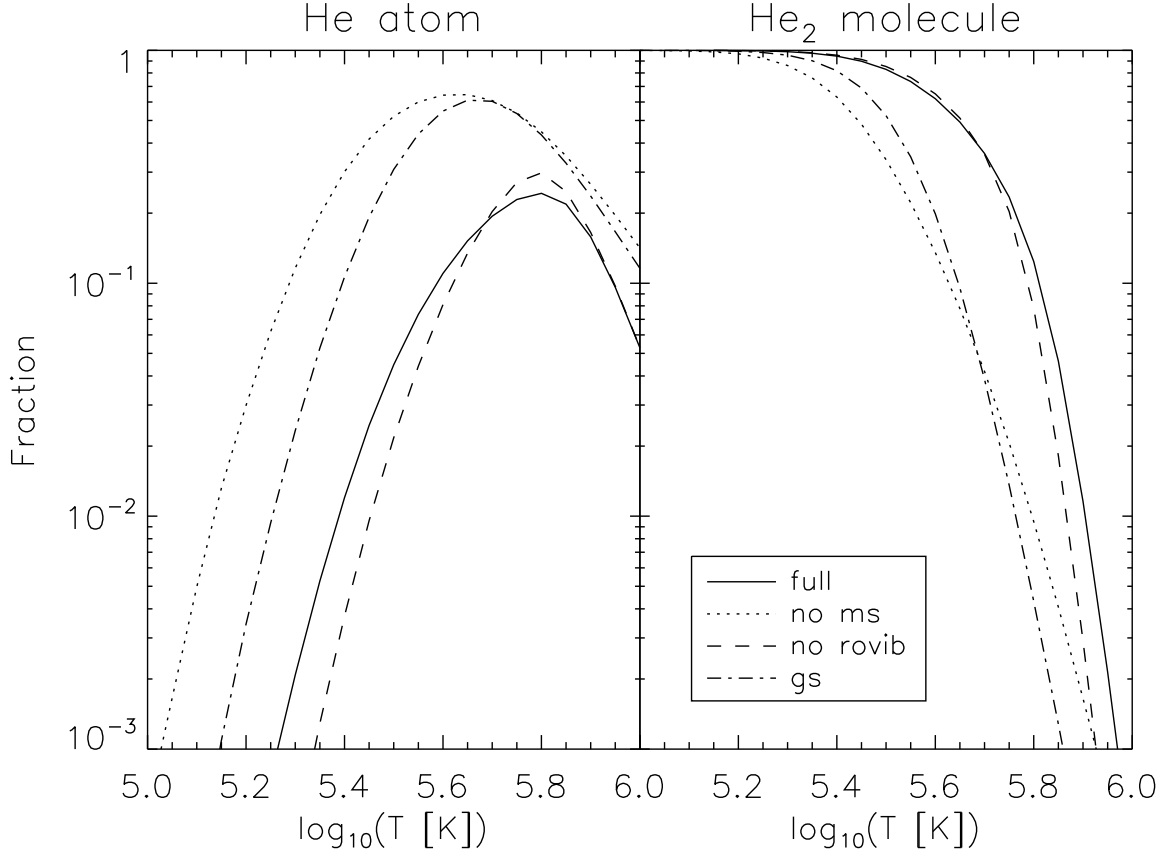


Fig. 9.— Fraction of helium atoms (left) and helium molecules (right)  $\rho = 10^2$  g/cm<sup>3</sup> at  $B = 10^{13}$  G. The solid lines show the results by taking into account all the physical effects discussed in this paper. The dotted and dashed lines ignored motional Stark effects and rovibrational states respectively. The dot-dashed lines include only the ground states.

(van Kerkwijk & Kaplan 2006). Timing analysis suggests that a couple of RQNS have dipole magnetic field strengths in the range of  $B = 10^{13}$ – $10^{14}$  G (Kaplan & van Kerkwijk 2005). Therefore, we investigated the ionization/dissociation balance of a helium atmosphere at  $B = 3 \times 10^{13}$  G. Figure 11 shows the contours of He<sup>+</sup> and He molecular fractions at  $3 \times 10^{13}$  G. He<sup>+</sup> is dominant at  $T \sim 10^6$  K and molecules become largely populated at  $T \lesssim 5 \times 10^5$  K.

Suppose all the RQNS have helium atmospheres on the surface. RQNS with higher temperatures ( $T \sim 10^6$  K) such as RXJ0720.4-3125 and RXJ1605.3+3249 will have He<sup>+</sup> ions predominantly with a small fraction of He atoms. Indeed, several bound-bound transition lines of He<sup>+</sup> ion have energies at the observed absorption line location at  $B \gtrsim 10^{13}$  G (Pavlov

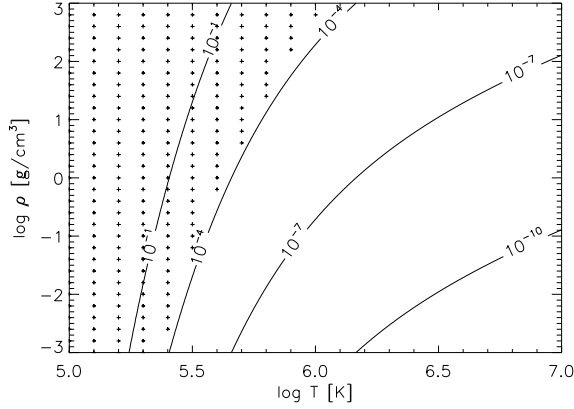


Fig. 10.— Ratio of  $\text{He}_3$  with respect to  $\text{He}_2$  at  $B = 10^{13}$  G (solid curve contours). The dotted area shows the  $(\rho, T)$  regime where a fraction of diatomic helium molecular ions is larger than 10%.

& Bezchastnov 2005). On the other hand, RQNS with lower temperatures ( $T \sim 5 \times 10^5$  K) such as RXJ0420.0-5022 may have some fraction of helium molecules, although the  $\text{He}^+$  ion is still predominant at low densities where absorption lines are likely formed.

## 6.2. 1E1207.4-5209

1E1207.4-5209 is a hot isolated NS <sup>4</sup> with age  $\sim 7 \times 10^3$  yrs. The fitted blackbody temperature is  $\sim 2 \times 10^6$  K (Mori et al. 2005). Presence of a non-hydrogenic atmosphere has been suggested since 1E1207 shows multiple absorption features at higher energies than hydrogen atmosphere models predicted (Sanwal et al. 2002; Hailey & Mori 2002; Pavlov & Bezchastnov 2005; Mori & Hailey 2006). Sanwal et al. (2002) interpreted the observed features as bound-bound transition lines of a  $\text{He}^+$  ion at  $B = 2 \times 10^{14}$  G. Also, Turbinner (2005) suggested that  $\text{He}_2^{3+}$  molecular ion may be responsible for one of the absorption features observed in 1E1207 at  $B \sim 4.4 \times 10^{13}$  G.

However, our study shows that the fraction of  $\text{He}_2^{3+}$  molecular ions is negligible at any B-field and temperature because more neutral molecular ions have significantly larger binding energies. We also investigated ionization/dissociation balance of helium atmospheres at  $2 \times 10^{14}$  G (figure 12). At  $B > B_Q$ , our scheme of treating finite nuclear mass effects

---

<sup>4</sup>Recent timing analysis suggests that 1E1207 is in a binary system (Woods et al. 2006). However, it is unlikely that 1E1207 is an accreting NS.

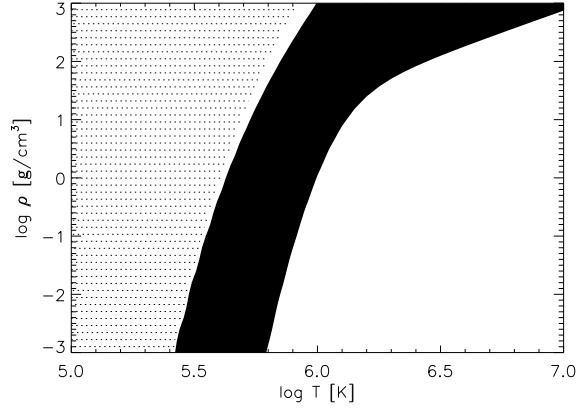


Fig. 11.— Ionization and dissociation balance of helium at  $B = 3 \times 10^{13}$  G. The dotted area is where the fraction of helium molecules and molecular ions (including  $\text{He}_2$ ,  $\text{He}_2^+$ ,  $\text{He}_2^{2+}$  and  $\text{He}_2^{3+}$ ) becomes more than 50%. The black area is where the fraction of  $\text{He}^+$  becomes more than 50%. The white region on the right is where the fraction of bare helium ions becomes more than 50%. In the narrow white region between the dotted and black area, atomic helium is somewhat abundant, so neither molecular nor singly ionized helium dominates

becomes progressively inaccurate. As a result, the ionization energy of helium atoms becomes significantly smaller and the  $\text{He}_2$  molecule becomes auto-ionized due to the  $m\hbar\Omega_B$  term discussed in §4.1. Therefore, the molecular fraction will be underestimated in this case (the left panel in figure 12). On the other hand, when we ignore the finite nuclear effects (the right panel in figure 12), the molecular fraction is likely overestimated. We expect that a realistic ionic and molecular fraction will be somewhere between the two cases. It is premature to conclude whether  $\text{He}^+$  is dominant for the case of 1E1207 since we do not have a self-consistent temperature and density profile. The study of ML06 and Lai (2001) also suggests the critical temperature below which helium molecule chains form is  $\sim 2 \times 10^6$  K at  $B = 2 \times 10^{14}$  G. This is close to the blackbody temperature of 1E1207. Further detailed studies are necessary to conclude the composition of helium atmospheres at  $B = 2 \times 10^{14}$  G.

## 7. Discussion

We have examined the ionization-dissociation balance of the helium atmospheres of strongly magnetized neutron stars. As the observational data on isolated neutron stars has improved over the past decade (Sanwal et al. 2002; Hailey & Mori 2002; van Kerkwijk & Kaplan 2006), both hydrogen and iron atmospheres have lost favour, and atmospheres



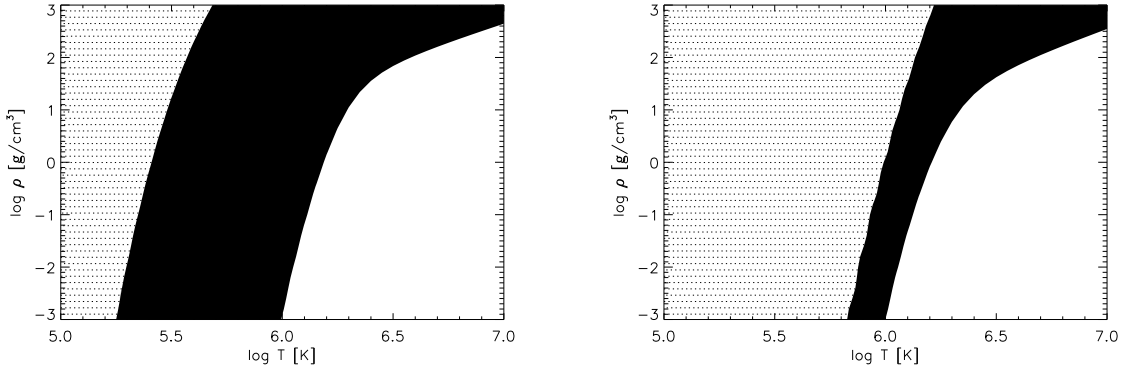


Fig. 12.— Ionization and dissociation balance of helium at  $B = 2 \times 10^{14}$  G. The left and right figure show the results with and without the finite nuclear mass effects respectively. In the dotted region the molecular and molecular ion fraction exceeds one half. In the black region singly ionized atomic helium dominates, and the white region demarcates fully ionized helium.

composed of heavier elements have been invoked to interpret both the continuum and spectral properties of neutron stars. On the other hand the theoretical investigations of Chang et al. (2004) and Chang & Bildsten (2004) have shown that diffusive nuclear burning may quickly deplete the hydrogen by so the NS surface may be composed of helium or heavier elements.

The dramatic results found here indicate several avenues for future work. Although the treatment of finite mass effects is problematic in the strong field limit, only by including this accurately can we know the physical state of matter in super-critical magnetic fields – solid, liquid or gas. The state can have dramatic effects of the outgoing radiation from these objects. It is also important to repeat a similar calculation to that presented here for molecular chains, including all of the relevant degrees of freedom of the chains, *i.e.* including the bending modes which were neglected here. Regardless, the high abundance of molecules under the conditions of observed neutron star atmospheres is bound to spur additional research into the statistical mechanics of highly magnetized molecules and polymers.

At the temperatures and densities of neutron star atmospheres the rotovibrational excitations of helium molecules are populated. Including these excitations increases the expected abundance of molecules by up to two orders of magnitude relative to calculations that ignore the internal states of the molecule. If helium comprises the atmospheres of isolated neutron stars, clearly it is crucial to understand the structure of helium molecules and molecular chains in order to interpret the spectra from neutron stars.

This work was supported in part by a Discovery Grant from NSERC (JSH). This work made use of NASA’s Astrophysics Data System. The authors were visitors at the Pacific Institute of Theoretical Physics during the nascent stages of this research.

## REFERENCES

- Alcock, C. & Illarionov, A. 1980, *ApJ*, 235, 534
- Angelie, C. & Deutch, C. 1978, *Phys. Lett. A*, 67, 353
- Bezchastnov, V. G., Pavlov, G. G., & Ventura, J. 1998, *Phys. Rev. A*, 58, 180
- Chang, P., Arras, P., & Bildsten, L. 2004, *ApJ*, 616, L147
- Chang, P. & Bildsten, L. 2004, *ApJ*, 605, 830
- Demeur, M., Heenen, P. ., & Godefroid, M. 1994, *Phys. Rev. A*, 49, 176
- Haberl, F., Schwope, A. D., Hambaryan, V., Hasinger, G., & Motch, C. 2003, *A&A*, 403, L19
- Haberl, F., Zavlin, V. E., Trümper, J., & Burwitz, V. 2004, *A&A*, 419, 1077
- Hailey, C. J. & Mori, K. 2002, *ApJ*, 578, L133
- Herold, H., Ruder, H., & Wunner, G. 1981, *Journal of Physics B Atomic Molecular Physics*, 14, 751
- Kaplan, D. L. & van Kerkwijk, M. H. 2005, *ApJ*, 635, L65
- Khersonskii, V. K. 1984, *Ap&SS*, 98, 255
- . 1985, *Ap&SS*, 117, 47
- Lai, D. 2001, *Rev. Mod. Phys.*, 73, 629
- Lai, D. & Salpeter, E. E. 1995, *Phys. Rev. A*, 52, 2611
- . 1996, *Phys. Rev. A*, 53, 152
- . 1997, *ApJ*, 491, 270
- Lai, D., Salpeter, E. E., & Shapiro, S. L. 1992, *Phys. Rev. A*, 45, 4832

- Medin, Z. & Lai, D. 2006a, submitted to Phys. Rev. A (astro-ph/0607166)
- . 2006b, submitted to Phys. Rev. A (astro-ph/0607277)
- Mori, K., Chonko, J. C., & Hailey, C. J. 2005, ApJ, 631, 1082
- Mori, K. & Hailey, C. J. 2002, ApJ, 564, 914
- . 2006, ApJ, 648, 1139
- Morse, P. M. 1929, Physical Review, 34, 57
- Neuhauser, D., Koonin, S. E., & Langanke, K. 1987, Phys. Rev. A, 36, 4163
- Pavlov, G. G. & Bezchastnov, V. G. 2005, ApJ, 635, L61
- Pavlov, G. G. & Meszaros, P. 1993, ApJ, 416, 752
- Potekhin, A. Y. 1994, J. Phys. B, 27, 1073
- . 1998, J. Phys. B, 31, 49
- Potekhin, A. Y., Chabrier, G., & Gilles, D. 2002, Phys. Rev. E, 65, 36412
- Romani, R. W. 1987, ApJ, 313, 718
- Sanwal, D., Pavlov, G. G., Zavlin, V. E., & Teter, M. A. 2002, ApJ, 574, L61
- Turbiner, A. V. 2005, preprint (astro-ph/0506677)
- Turbiner, A. V., Guevara, N. L., & López Vieyra, J. C. 2006, preprint (physics/0606083)
- Turbiner, A. V. & López Vieyra, J. C. 2003, Phys. Rev. A, 68, 012504
- van Kerkwijk, M. H. & Kaplan, D. L. 2006, preprint (astro-ph/0607320)
- van Kerkwijk, M. H., Kaplan, D. L., Durant, M., Kulkarni, S. R., & Paerels, F. 2004, ApJ, 608, 432
- Vincke, M., LeDourneuf, M., & Baye, D. 1992, Journal of Physics B Atomic Molecular Physics, 25, 2787
- Woods, P. M., Zavlin, V. E., & Pavlov, G. G. 2006, preprint (astro-ph/0608483)